AIP Journal of Applied Physics

Tunneling through InAs quantum dots in AlGaAs/GaAs double barrier resonant tunneling diodes with InGaAs quantum well emitters

S. D. Lin and C. P. Lee

Citation: Journal of Applied Physics **93**, 2952 (2003); doi: 10.1063/1.1543631
View online: http://dx.doi.org/10.1063/1.1543631
View Table of Contents: http://scitation.aip.org/content/aip/journal/jap/93/5?ver=pdfcov
Published by the AIP Publishing

Tunneling through InAs quantum dots in AlGaAs/GaAs double barrier resonant tunneling diodes with InGaAs quantum well emitters

S. D. Lin and C. P. Lee[a]
Department of Electronics Engineering, National Chiao Tung University, 1001 Ta Hsueh Road, Hsinchu, Taiwan, Republic of China

(Received 23 July 2002; accepted 11 December 2002)

Using InGaAs quantum well emitters, AlGaAs/GaAs double barrier resonant tunneling diodes with and without self-assembled InAs/GaAs quantum dots (QDs) have been studied extensively. Because the energy state of the emitter was lower than the level of the ground state within InAs QDs, the resonant tunneling was observed clearly near zero bias in all devices. From the results of bias-dependent photoluminescence and current–voltage characteristics, we obtain unambiguously the resonant tunneling through the InAs QDs, both controllably and reproducibly. © *2003 American Institute of Physics.* [DOI: 10.1063/1.1543631]

I. INTRODUCTION

Discrete energy levels and atom-like behaviors in semiconductor quantum dots (QDs) and devices utilizing such properties have attracted much interest in recent years.[1] Among the various methods of fabricating quantum dots, self-assembly growth of InAs dots in GaAs is the most popular and the simplest way to produce high quality dots and devices. Usually, the experimental studies of the quantized states in the quantum dots rely on optical methods. Recently, the states in QDs and the transport characteristics were studied by means of resonant tunneling through the dots.[2–4] These properties are important to both fundamental physics and nano-device applications. However, in a conventional double barrier resonant tunneling structure, the ground state energy of InAs QDs in GaAs or AlAs matrix is usually lower than the emitter energy level, making it difficult to observe the tunneling phenomena through the QDs.[5] The reported results, therefore, vary from device to device and suffer from the reproducibility problem. It sometimes remains questionable whether the tunneling comes from the states in QDs, or from other impurity or defect related states.

In this work, we proposed a structure to overcome the difficulty mentioned above. In a conventional resonant tunneling diode (RTD) with InAs QDs, the emitters are GaAs, and the barriers are AlGaAs or AlAs. [see Fig. 1(a)] Because the band gap energy of InAs is so much lower than that of the barriers, the quantized energy levels of QDs are lower than that of the GaAs emitter. Only a small portion of the inhomogeneous QDs may have energy levels high enough to be involved in the tunneling processes. This is easily understandable with the help of the flatband diagram shown in Fig. 1(a). In this work, InGaAs quantum wells (QWs) were used as the emitters to lower the energy [see Fig. 1(b)] so most of the InAs QDs can be involved in the tunneling processes. Detailed studies by temperature dependent $I-V$ measurement and bias-dependent photoluminescence (PL) are presented in the following. From the result and discussion, we believe the tunneling through InAs QDs has been achieved ambiguously.

II. SAMPLE GROWTH, DEVICE PROCESS, AND CHARACTERIZATION

The RTD structure, shown in Fig. 2, was grown on a (100)n^+-GaAs substrate by a Varian Gen II molecular beam epitaxy system. Aside from the N+ contact layers, the middle *i* region consists of a 1.5 nm GaAs/2 ML InAs/3.5 nm GaAs well sandwiched between two 7 nm $Al_{0.3}Ga_{0.7}As$ barriers, and two 12 nm $In_{0.21}Ga_{0.79}As$ emitters and two 15 nm undoped GaAs spacer layers. For comparison, another sample with the same structure but without InAs QDs inside was also grown under the same growth conditions.

The density of the quantum dots was about $4\times10^{10}\,cm^{-2}$ measured by an atomic force microscope (AFM). The measured PL result of the unprocessed sample with QDs at 25 K shows that the PL peak energy of the InGaAs QWs (1.298 eV) is lower than that of the InAs QDs (1.348 eV). This is important to our experiment because we want to make sure that the electrons from the emitter can resonant tunnel through the ground states of the QDs. After growth, the RTD devices were fabricated with conventional lithography and metalization processes. The mesa area for each RTD was $180\times180\ \mu m^2$. To measure the photoluminescence under electric field, we fabricated some devices with windows on the top metal contact. In those devices, the mesa and window sizes were 320×220 and $180\times180\ \mu m^2$, respectively.

III. RESULT AND DISCUSSION

A. Resonant tunneling through two-dimensional states in well

The temperature dependent $I-V$ characteristics of the RTD devices with and without QDs are shown in Figs. 3(a) and 3(b), respectively. Clear negative differential resistances (NDRs), which are due to resonant tunneling through the quantum well states in the middle layer, were observed in both samples even at room temperature. Comparing Figs.

[a]Electronic mail: cplee@cc.nctu.edu.tw

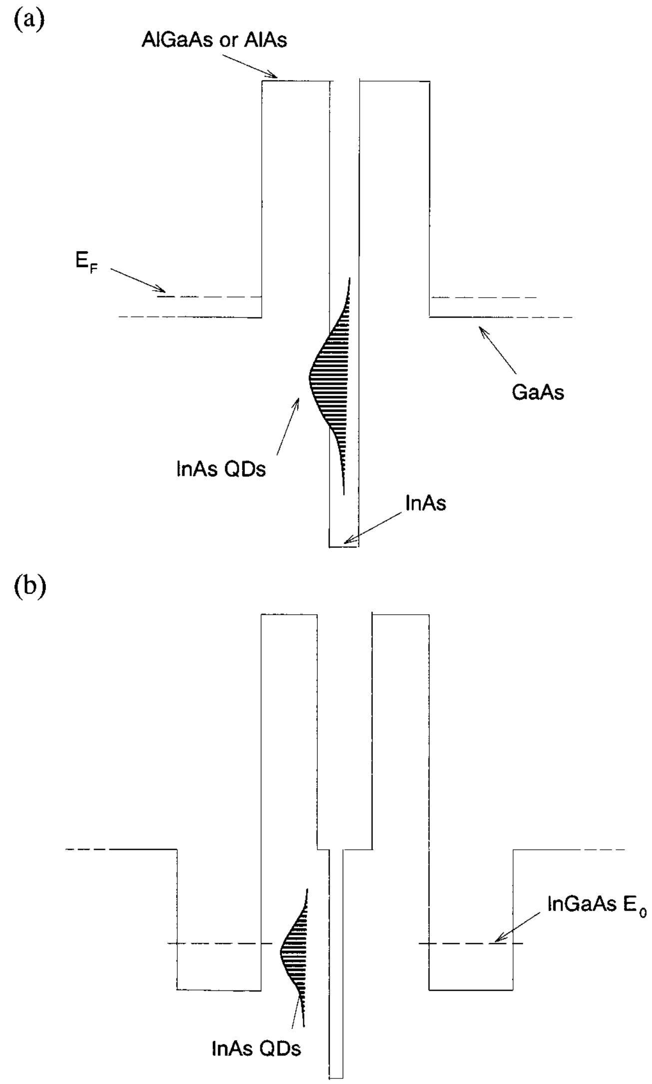

FIG. 1. The flatband diagrams for the conventional (a), and proposed (b) structures of the resonant tunneling diodes with QDs.

600nm n^+-GaAs ($n^+=2\times10^{18}cm^{-3}$)
15nm i-GaAs
12nm i-$In_{0.21}Ga_{0.79}As$
7nm i-$Al_{0.3}Ga_{0.7}As$
3.5nm i-GaAs
0ML or 2ML InAs
1.5nm i-GaAs
7nm i-$Al_{0.3}Ga_{0.7}As$
12nm i-$In_{0.21}Ga_{0.79}As$
15nm i-GaAs
~ 200nm n^+-GaAs buffer ($2\times10^{18}cm^{-3}$)
(100) n^+-GaAs substrate

FIG. 2. Layer structure of the samples studied.

3(a) and 3(b), we see that the overall $I-V$ curves are very similar, except that the resonant peaks of the device with QDs occur at lower biases. Similar phenomena have been observed in Ref. 4. This result can be understood with the help of Fig. 4. Because of the presence of the wetting layer (WL), the lowest two-dimensional (2D) state in the well region shifts downward. So the resonant tunneling happens at smaller bias voltages for the devices with QDs. Based on simple calculations, for the sample without QDs, there is only one confined state in the well and the resonant tunneling is caused by this state. But for the sample with QDs, there is an additional state in the thin wetting layer and so the resonant tunneling occurs at a lower bias voltage.

In order to understand the source state in emitters that contributes to resonant tunneling, we analyzed the temperature dependence of peak-to-valley current ratio (PVCR), peak current (I_p), and valley current (I_v) for the NDRs. Both samples with and without QDs have similar characteristics. Figure 5 shows the result for a device without QDs. Unlike the conventional RTDs where both the peak current and the peak-to-valley current ratio increase when temperature is lowered, the peak current decreases as the temperature is lowered, and the PVCR has a maximum value at around 150 K. This result is an indication that the NDRs in the $I-V$ curves are due to resonant tunneling from the excited states in the emitter, as suggested in Ref. 7. Because the electron population in the excited state increases with device temperature, the peak current drops as the temperature decreases. The PVCR, on the other hand, depends on the peak current and the carrier scattering, which is reduced when the temperature is reduced. Combing these two effects, the highest PVCR occurs at a medium temperature. We have theoretically calculated the energy states in the InGaAs QW emitters. Indeed there are two confined electron states in the well. The ground state and the first excited state locate at 52 and 5 meV below the conduction band edge of GaAs.

To understand the states contributing to the NDRs, we also measured the photoluminescence of the device with QDs under an external bias.[6] Figure 6 shows the measured PL spectra under a 10 mW excitation power at $T=25$ K. At zero bias, three PL peaks originated from n^+-GaAs, InAs QDs and InGaAs QWs are observed. When the device is positively biased (meaning the electrons enter the device from the substrate side), the signal from the InAs wetting layer (at around 850 nm) appears when the voltage is above 0.3 V. When the device is negatively biased, however, no signal around 850 nm is observed. The difference comes from the asymmetry in the barrier structure for the wetting layer. As shown in Fig. 2, the GaAs layer below (above) the InAs layer is 1.5 nm (3.5 nm). So, when electrons come from the bottom side (positive bias), it is easier for the electrons to tunnel through the barrier and accumulate in the 2D state in the wetting layer as compared with the case when the electrons enter the well from the top electrode. As a result, the PL signal from the wetting layer state is reduced when the device is negatively biased. Besides the InAs wetting layer emission, the emission peak from the InGaAs emitters (around 960 nm) is also not symmetrical in the spectra shown in Fig. 6. When the device is negatively biased, the InGaAs emission peak broadens on the higher energy side and merges with the PL signal of QDs. Because the thick n^+-GaAs contact layer (about 600 nm) absorbs most of the

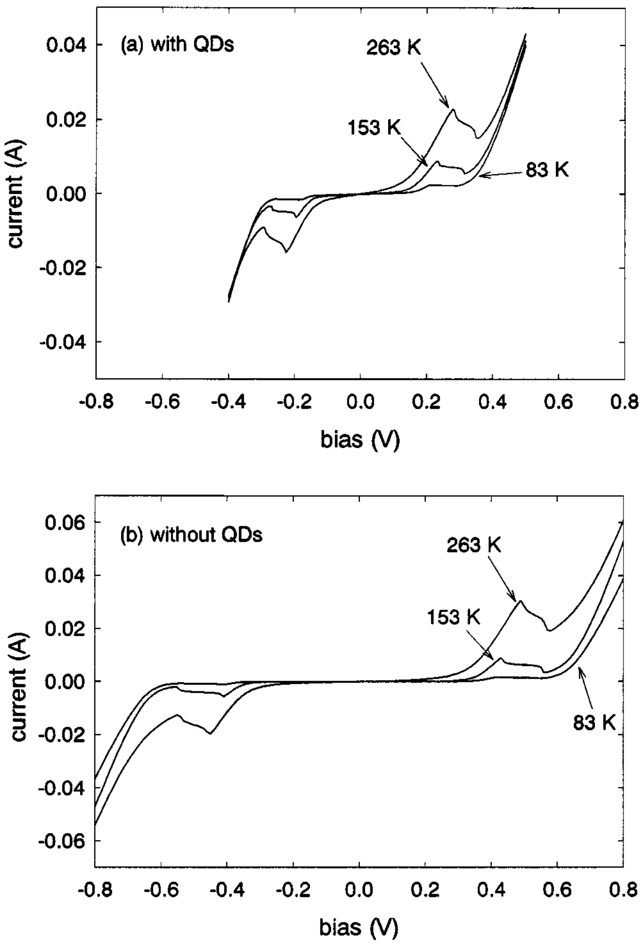

FIG. 3. Temperature dependent $I-V$ characteristics of the RTDs with QDs (a), and without QDs (b).

incident light from the pumping laser, the emission from the upper InGaAs QW is stronger than that from the bottom InGaAs QW. When the upper electrode is negatively biased, electrons fill not only the ground state but also the excited state in the upper InGaAs emitter, so the extended tail on the

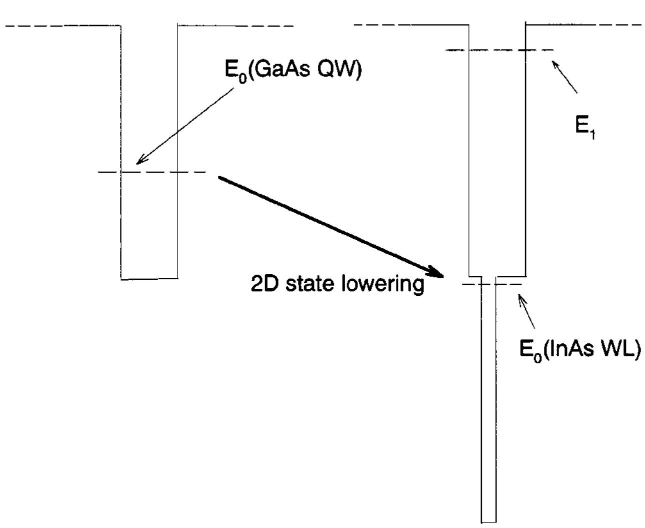

FIG. 4. Schematic band diagram for the 2D state lowering due to the insertion of InAs layer.

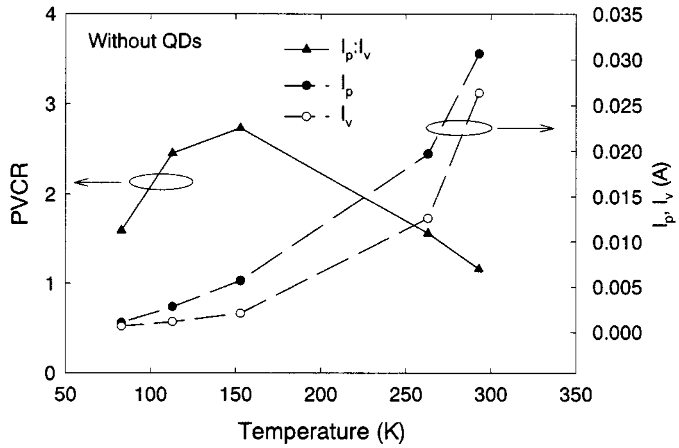

FIG. 5. Temperature dependent peak current (I_p), valley current (I_v), and peak-to-valley current ratio (PVCR) for the RTDs without QDs.

higher energy side is observed. On the other hand, when the device is positively biased, the upper InGaAs QW becomes the collector and the higher energy state is unoccupied. Therefore, the InGaAs emission peak is only due to the ground state in the QW and the PL signal becomes narrow.

B. Resonant tunneling through QD states

If we lower the measurement temperature and expand the $I-V$ curves near zero bias, we can see a very interesting difference between the sample with and without InAs QDs. Figure 7. shows the differential resistance (dV/dI) of two samples at 32 K. A very clear dip near zero bias is observed in the curve of the sample with QDs. This result is observed in all devices with QDs (see inset of Fig. 7). However, for the devices without QDs, such a feature is never observed.

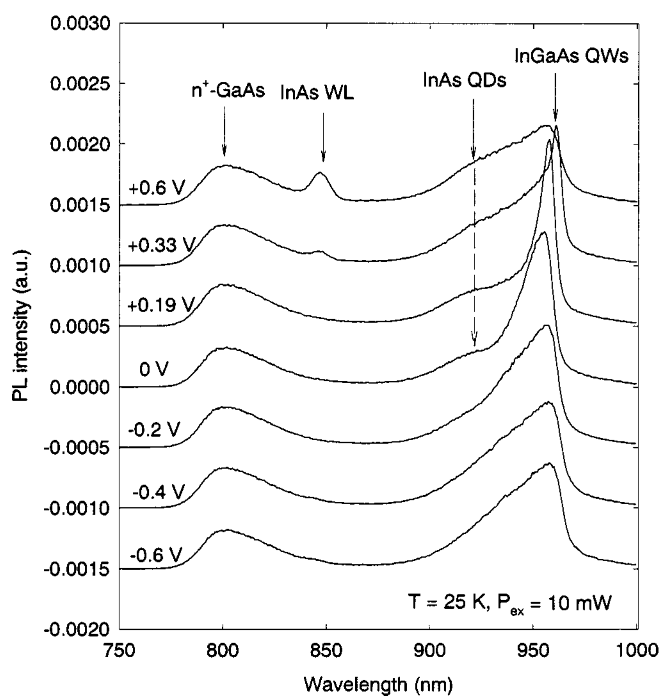

FIG. 6. Bias-dependent photoluminescence results of the RTDs with QDs; the curves were shifted vertically for clarity.

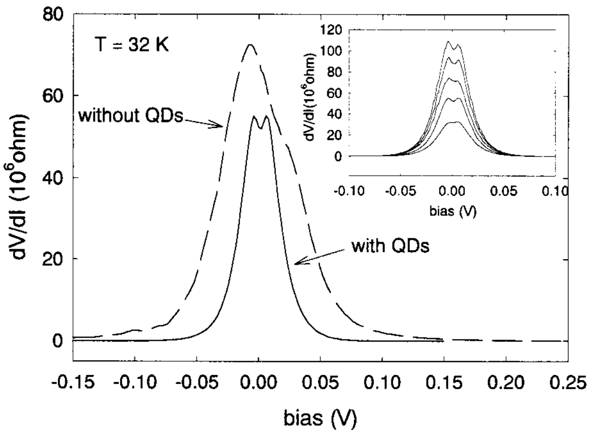

FIG. 7. The dV/dI characteristics of the RTDs with and without QDs. The inset shows the characteristics of individual devices with QDs.

So clearly, the dip in the differential resistance is a result of resonant tunneling through the InAs quantum dots.

We have calculated the energy states for both structures. The result is shown in the flatband diagrams in Figs. 8(a) and 8(b). The level of zero energy is aligned with the conduction band edge of bulk GaAs. There are two states in the InGaAs QW emitters, located at -52 and -5 meV. For the sample without QDs, Fig. 8(a), there is only one resonant state in the well region, located at $+76$ meV. For our samples, the energy-voltage conversion factor α is about 0.21, which is calculated by the ratio of the distance between the middle of InGaAs QW and GaAs QW (15.5 nm) and the thickness of the undoped region (73 nm). Using the factor α=0.21, and the energy difference between the first excited state and the resonant state in the well (81 meV), we get the NDR bias voltage being 386 meV, very close to the measured 395 meV in Fig. 3(b). For the sample with QDs, the flatband diagram is shown in Fig. 8(b). We can estimate the energy levels for InAs QDs and InAs WL using the measured PL peaks of 1348 and 1458 meV from the zero-bias PL spectrum in Fig. 6. The energy level of the WL state can be calculated according to Grundmann's work.[8] On the other hand, from our measured AFM image of the uncapped QDs grown under the same condition (not shown here), the base and height of the QDs were about 20–25 and 2.0–2.5 nm respectively, close to the lens shape calculated by Williamson, Wang, and Zunger in Ref. 9. Based on their calculated result, the ratio between ΔE_c and ΔE_g for QDs is about 50%. So we can obtain the energy levels of QDs and WL at approximately 85 and 12 meV below the conduction band edge of GaAs, respectively. From the flatband diagram in Fig. 8(b), we can see that the energy level of E_1 in the InGaAs QW emitters nearly aligns with that of the InAs WL state. However, from Fig. 3(a), we can see that the NDRs from the tunneling between E_1 and WL occur at about 195 mV. This is understandable if we consider the charging effect in the well region. The additional space charges in the well region lift up the states in the well. Using the conversion factor α and the NDR voltage, we estimate the uplift energy to be as large as 48 meV. As shown in Fig. 8(b), including this lift in QD states, the energy level of InGaAs E_0 state is about 15 meV below the QD states, as indicated with the lower dash line. So, it is why the resonant tunneling from InGaAs E_0 states through QD states is observed near zero bias, as shown in Fig. 7.

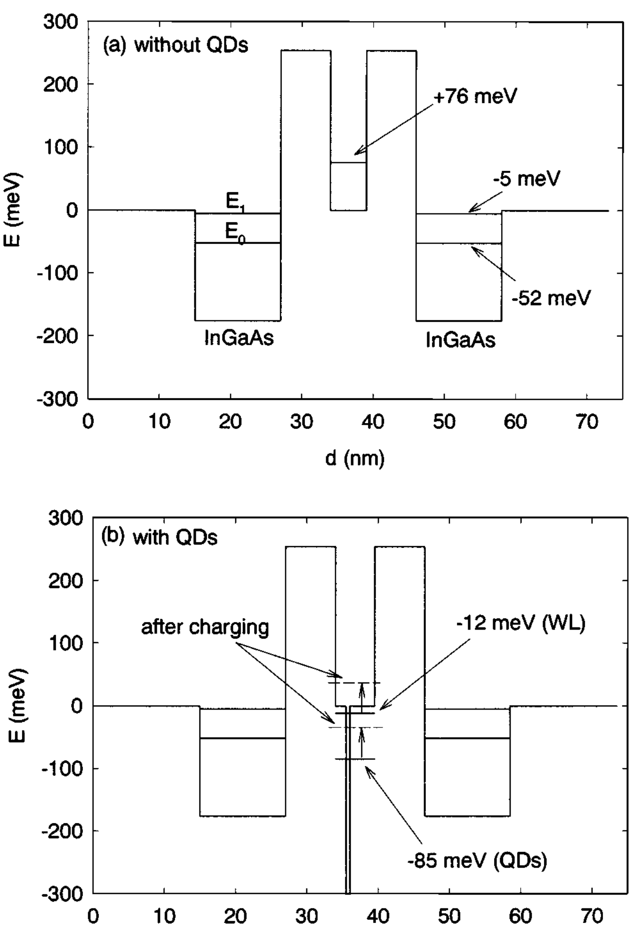

FIG. 8. Calculated flatband diagrams for the RTDs without QDs (a), and with QDs (b).

As stated above, the charging effect in QDs lifts up the states' level in the well region. The exact lift-up energy and the band diagram need self-consistent calculation considering the tunneling probability, capture rate, and exact location of electron distribution and wave function of QDs, that is out of the scope of this article. However, if we consider the charging effect by a capacitor model, the dependence between charging density in the well region and the voltage difference between QDs and the InGaAs QWs could be estimated easily. The electric field between the layer of QDs and n^+-GaAs is $q\sigma/2\varepsilon$, where q is the electron charge, σ is the sheet density of charging electrons in well region and, ε is the effective dielectric constant. With the distance between the QD layer and the InGaAs QWs (15.5 nm), to build up a voltage difference of about 48 meV, which is extracted by NDR location, the sheet density of charging electrons has to be as large as $4\times10^{11}\,cm^{-2}$. It is about one order of magnitude larger than the QD density. This estimation shows that the most of charging electrons occupy the WL states (about 80%, assuming two electrons in each QD and there should be only one confined zero-dimensional state in conduction band for our QDs). It also explains the insensitivity of this charging effect, because most charging electrons reside in 2D WL states.

IV. CONCLUSION

We have extensively studied the AlGaAs/GaAs double barrier resonant tunneling diodes with InAs quantum dots and InGaAs quantum well emitters. Clear negative differential resistances (NDRs) were observed in both samples with and without InAs QDs. From the temperature dependent $I-V$ characteristics and bias-dependent luminescence spectra, we can conclude that the NDRs come from the resonant tunneling from the first excited state in the InGaAs QW emitter through the lowest 2D state in the well region. The measured peak voltage of the NDRs is consistent with the calculated value. Furthermore, near zero bias, a clear dip feature in the differential resistance was observed in the devices with InAs QDs at low temperatures. Combing the evidence of PL, temperature dependent $I-V$ curves, and the calculated flat-band diagrams, we can unambiguously conclude that the dip feature is the resonant tunneling from the ground state of the InGaAs QW emitter through the InAs QDs.

ACKNOWLEDGMENTS

This work was supported by the National Science Council under Contract No. NSC 90-2215-E-009-013 and the Lee-MTI center of National Chiao Tung University. The authors also want to thank Dr. J. S. Wu from Procomp Information Ltd. for helpful discussion.

[1] M. A. Reed, J. N. Randall, R. J. Aggarwal, R. J. Matyi, T. M. Moore, and A. E. Wetsel, Phys. Rev. Lett. **60**, 535 (1988).
[2] I. E. Itskevich, T. Ihn, A. Thornton, M. Henini, T. J. Foster, P. Moriarty, A. Nogaret, P. H. Beton, L. Eaves, and P. C. Main, Phys. Rev. B **54**, 16401 (1996).
[3] T. Suzuki, Y. Haga, K. Nomoto, K. Taira, and I. Hase, Solid State Electron. **42**, 1303 (1998).
[4] A. Patane, A. Polimeni, L. Eaves, P. C. Main, M. Henini, Yu. V. Dubrovskii, A. E. Belyaev, P. N. Brounkov, E. E. Vdovin, and Y. N. Khanin, J. Appl. Phys. **88**, 2005 (2000).
[5] J. Wang, R. Li, Y. Wang, W. Ge, and D. Z.-Y. Ting, Microelectron. Eng. **43,44**, 341 (1998).
[6] J. F. Young, B. M. Wood, G. C. Aers, R. L. S. Devine, H. C. Liu, D. Landheer, M. Buchanan, A. J. Spring Thorpe, and P. Mandeville, Phys. Rev. Lett. **60**, 2085 (1988).
[7] J. S. Wu, C. Y. Chang, C. P. Lee, K. H. Chang, D. G. Liu, and D. C. Liou, Appl. Phys. Lett. **57**, 2311 (1990).
[8] M. Grundmann, O. Stier, and D. Bimberg, Phys. Rev. B **52**, 11969 (1995).
[9] A. J. Williamson, L. W. Wang, and A. Zunger, Phys. Rev. B **62**, 12963 (2000).